ANZIAM J. **63** (2021), 39–57
doi:10.1017/S1446181121000031

STOCHASTIC MODEL PREDICTIVE CONTROL FOR SPACECRAFT RENDEZVOUS AND DOCKING VIA A DISTRIBUTIONALLY ROBUST OPTIMIZATION APPROACH

ZUOXUN LI[1] and KAI ZHANG[✉2]

(Received 17 May, 2020; accepted 10 November, 2020; first published online 19 April, 2021)

Abstract

A stochastic model predictive control (SMPC) algorithm is developed to solve the problem of three-dimensional spacecraft rendezvous and docking with unbounded disturbance. In particular, we only assume that the mean and variance information of the disturbance is available. In other words, the probability density function of the disturbance distribution is not fully known. Obstacle avoidance is considered during the rendezvous phase. Line-of-sight cone, attitude control bandwidth, and thrust direction constraints are considered during the docking phase. A distributionally robust optimization based algorithm is then proposed by reformulating the SMPC problem into a convex optimization problem. Numerical examples show that the proposed method improves the existing model predictive control based strategy and the robust model predictive control based strategy in the presence of disturbance.

2020 *Mathematics subject classification*: primary 93B45; secondary 49N10.

Keywords and phrases: stochastic model predictive control, rendezvous and docking, Monte Carlo..

1. Introduction

1.1. Background In modern aerospace engineering, autonomous spacecraft rendezvous and docking manoeuvres are the most important components, which have been used on many occasions. For example, the International Space Station (ISS) is so huge that the launch vehicle can only launch it in batches and then use the rendezvous and docking manoeuvres to assemble it. So, the rendezvous and docking manoeuvres are the foundation for the construction of the ISS. These are also used in

[1]The College of Electrical Engineering, Sichuan University, 610065 Chengdu, China;
e-mail: lizuoxun@stu.scu.edu.cn
[2]The College of Electrical Engineering, Southwest Jiaotong University, 610031 Chengdu, China;
e-mail: kaizhang@swjtu.edu.cn

other space missions, such as the transportation of astronauts, supplies to long-term orbiting space stations, the exchange of visits between orbiting spacecraft, material transfer, emergency life saving, and docking between spacecraft and space station to perform a series of maintenance tasks [25].

1.2. Literature review In the past decades, the control of spacecraft rendezvous and docking has been intensively studied [1, 12, 17, 19–22]. A comprehensive overview of the programmes, missions, and techniques that have come to define orbital rendezvous was provided by Fehse [12]. The optimal control [20] and adaptive sliding mode control [19] have been used in spacecraft rendezvous and docking. Some works focus on different missions, such as spacecraft rendezvous and docking in an elliptical orbit and incorporating spacecraft rendezvous and docking capability into spacecraft flying in formation [22].

However, there exist many constraints during the process of spacecraft rendezvous and docking, and the above methods cannot deal with the constraints properly. To address this problem, model predictive control (MPC) was introduced. MPC possesses some attractive characteristics as a candidate for the guidance and control framework. Firstly, MPC replans the optimal trajectory at each sampling instant [7]. Secondly, due to the implicit way in which the MPC problem is specified, carrying an exhaustive library of manoeuvres for every possible initial configuration is not necessary. Thirdly, the intrinsic ability of MPC to handle constraints makes it a logical choice for rendezvous and docking. MPC is also inherently reconfigurable. Constraints (for example, thrust availability and passive safety requirements) and model parameters (for example, target orbit) can be modified on-line; this is an attractive feature if these are not known exactly until the target has been detected.

The control of spacecraft rendezvous with stable attitude or spinning targets in an elliptical orbit was provided by Li and Zhu [18]. The two cases of a nonrotating and a rotating (tumbling) platform, treated separately, were provided by Cairano et al. [4], and trajectories were evaluated in terms of manoeuvre time and fuel consumption. It was demonstrated that MPC can be an effective feedback control approach to satisfy various manoeuvre requirements, reduce fuel consumption, and provide robustness to disturbances. The design and implementation of an MPC system [15] was presented to guide and control a tracking spacecraft during rendezvous with a passive target spacecraft in an elliptical or circular orbit, from the point of target detection all the way to capture. A method that directly optimizes the final spacecraft rendezvous precision without restricting the duration of the manoeuvres was provided by Deaconu et al. [10], and that method is based on feedback from MPC. The so-called chance-constrained model predictive control was provided by Gavilan et al. [13], who applied it to spacecraft rendezvous in the presence of model uncertainties and disturbances. A robust technology and mixed MPC (M-MPC) framework was provided by Zhu et al. [26], who combined them to form a robust M-MPC method to deal with the multi-step short range spacecraft rendezvous problem. A strategy and case study of spacecraft relative motion guidance and control, based on the application of linear quadratic MPC with dynamically reconfigurable constraints, was provided by Weiss et al. [23].

1.3. Contributions There are numerous phenomena that can disturb or perturb the rendezvous and docking process of spacecraft, for example, thrust perturbations and atmospheric drag in low orbit [13]. In the existing literature, disturbances are usually assumed to be bounded and then tackled by the worst-case robust optimization based approach [16]. However, it is not the case in practice since the bound cannot be measured. Moreover, worst-case robustness always leads to conservativeness in terms of performance.

Motivated by this fact, this paper revisits the MPC of spacecraft rendezvous and docking [23] in the presence of disturbances by using a distributionally robust optimization approach. The whole process of rendezvous and docking can be divided into distinct rendezvous and docking phases, and different types of constraints are required to be considered in each phase. For example, there are obstacle avoidance constraints during the rendezvous, and a soft docking constraint is considered during the docking phase, respectively. Thrust constraints have to be imposed during both of the two phases.

This work proposes the use of the stochastic model predictive control (SMPC) [2, 3, 8] as an alternative to design controllers for spacecraft, which is an improvement of robust model predictive control (RMPC). The purpose of the SMPC algorithm is to use the randomness and statistical characteristics of uncertain factors. In this framework, the objective function is in the form of expectation, and the hard constraints of system variables are re-expressed as chance constraints, allowing the system to violate the constraints under a given probability, so unbounded disturbances can be considered [11].

Compared with traditional MPC, SMPC has the ability to deal with disturbance and, compared with RMPC, due to the weaker conservatism, SMPC has better performance.

1.4. Organization The rest of this paper is organized as follows. Section 2 states the SMPC problem of spacecraft rendezvous and docking. Section 3 introduces the SMPC algorithm. Section 4 shows a Monte Carlo comparison of MPC, RMPC, and SMPC. Finally, we conclude the paper by making some concluding remarks in Section 5.

2. Problem statement

2.1. Dynamical system A tracking spacecraft is manoeuvred close to a target spacecraft in a nominal orbit. The target spacecraft is assumed to be at the origin of Hill's frame [24] as shown in Figure 1.

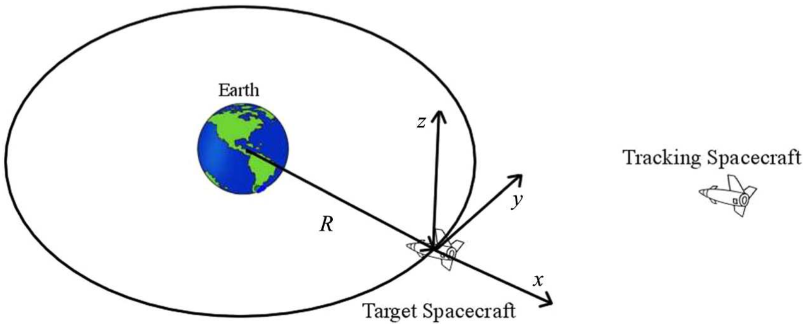

FIGURE 1. Hill's frame.

The relative motion of the tracking spacecraft to the target spacecraft on a circular orbit can be described by the following differential equations [9]:

$$\ddot{x} = 2n\dot{y} + n^2(R + x) - \mu \frac{R + x}{[(R + x)^2 + y^2 + z^2]^{3/2}} + \frac{F_x}{m_c},$$
$$\ddot{y} = -2n\dot{x} + n^2 y - \mu \frac{y}{[(R + x)^2 + y^2 + z^2]^{3/2}} + \frac{F_y}{m_c},$$
$$\ddot{z} = -\mu \frac{z}{[(R + x)^2 + y^2 + z^2]^{3/2}} + \frac{F_z}{m_c},$$

where x, y, and z are the components of the tracking spacecraft position relative to the target in Hill's frame, $n = \sqrt{\mu/R^3}$ is the angular speed of the target spacecraft's orbit, $\mu = 398600.4\ \mathrm{km}^3/\mathrm{s}^2$ is the gravitation parameter of the Earth, R is the orbit radius of the target spacecraft, F_x, F_y, and F_z are the forces of the tracking spacecraft in the x, y, and z axes, respectively, and m_c is the mass of the tracking spacecraft.

Suppose that the distance $d = \sqrt{x^2 + y^2 + z^2}$ between the tracking spacecraft and the target spacecraft is far less than R; then the well-known linearized Clohessy–Wiltshire–Hill (CWH) model (2.1)–(2.3) can be used here:

$$\ddot{x} - 3n^2 x - 2n\dot{y} = \frac{F_x}{m_c}, \tag{2.1}$$

$$\ddot{y} + 2n\dot{x} = \frac{F_y}{m_c}, \tag{2.2}$$

$$\ddot{z} + n^2 z = \frac{F_z}{m_c}. \tag{2.3}$$

To proceed further, we denote

$$u_x = \frac{F_x}{m_c}, \quad u_y = \frac{F_y}{m_c}, \quad u_z = \frac{F_z}{m_c}.$$

https://doi.org/10.1017/S1446181121000031 Published online by Cambridge University Press

In fact, u_x, u_y, and u_z are the accelerations of the tracking spacecraft in the x, y, and z directions, respectively. Then, by letting

$$\mathbf{x} = [x\ y\ z\ \dot{x}\ \dot{y}\ \dot{z}]^T, \quad \mathbf{u} = [u_x\ u_y\ u_z]^T$$

be the state vector and the control vector, respectively, the state space model of (2.1)–(2.3) can be written as

$$\dot{\mathbf{x}} = \mathbf{A}_c\mathbf{x} + \mathbf{B}_c\mathbf{u}, \tag{2.4}$$

where

$$\mathbf{A}_c = \begin{bmatrix} 0 & 0 & 0 & 1 & 0 & 0 \\ 0 & 0 & 0 & 0 & 1 & 0 \\ 0 & 0 & 0 & 0 & 0 & 1 \\ 3n^2 & 0 & 0 & 0 & 2n & 0 \\ 0 & 0 & 0 & -2n & 0 & 0 \\ 0 & 0 & -n^2 & 0 & 0 & 0 \end{bmatrix}, \quad \mathbf{B}_c = \begin{bmatrix} 0 & 0 & 0 \\ 0 & 0 & 0 \\ 0 & 0 & 0 \\ 1 & 0 & 0 \\ 0 & 1 & 0 \\ 0 & 0 & 1 \end{bmatrix}.$$

In order to develop an implementable MPC algorithm, a discrete system is required. To this end, we discretize the continuous-time system (2.4) with sampling time ΔT (in this paper, we set it to 20 s). Considering an external disturbance, the discretized system is

$$\mathbf{x}_{t+1} = \mathbf{A}\mathbf{x}_t + \mathbf{B}\mathbf{u}_t + \boldsymbol{\delta}_t, \tag{2.5}$$

where $\mathbf{A}$ and $\mathbf{B}$ are as in (2.6) and (2.7), respectively, $\mathbf{x}_t = [x_t, y_t, z_t, \dot{x}_t, \dot{y}_t, \dot{z}_t]^T$ is the state vector at time step $t \in \mathbb{Z}^+$, $\mathbf{u}_t = [u_{x,t}, u_{y,t}, u_{z,t}]^T$ is the control vector at time step $t \in \mathbb{Z}^+$, and $\boldsymbol{\delta}_t \in \mathbb{R}^{n_\omega}$ is the external disturbance vector. Particularly, the distribution of $\boldsymbol{\delta}_t$ is not exactly known. Only the mean $\boldsymbol{\mu}_0$ and the covariance matrix $\boldsymbol{S}_0$ are known to the controller. In addition, the following matrices $\mathbf{A} \in \mathbb{R}^{n_x \times n_x}$ and $\mathbf{B} \in \mathbb{R}^{n_x \times n_u}$ are known to the system:

$$\mathbf{A} = \begin{bmatrix} 4 - 3\cos(nT) & 0 & 0 & \sin(nT)/n & 2/n - 2\cos(nT)/n & 0 \\ 6\sin(nT) - 6nT & 1 & 0 & 2\cos(nT)/n - 2/n & 4\sin(nT)/n - 3T & 0 \\ 0 & 0 & \cos(nT) & 0 & 0 & \sin(nT)/n \\ 3n\sin(nT) & 0 & 0 & \cos(nT) & 2\sin(nT) & 0 \\ 6n\cos(nT) - 6n & 0 & 0 & -2\sin(nT) & 4\cos(nT) - 3 & 0 \\ 0 & 0 & -n\sin(nT) & 0 & 0 & \cos(nT) \end{bmatrix} \tag{2.6}$$

https://doi.org/10.1017/S1446181121000031 Published online by Cambridge University Press

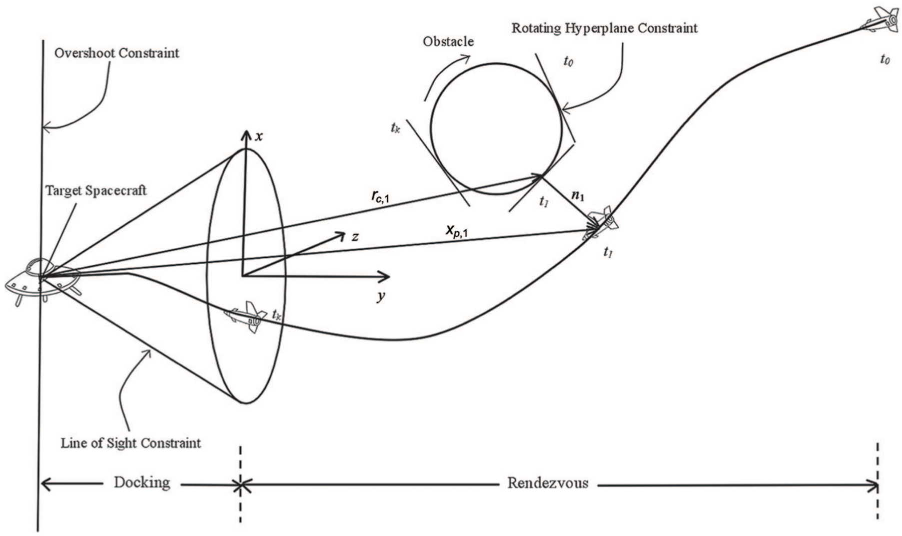

FIGURE 2. Schematic of a spacecraft docking manoeuvre subject to LoS, overshoot, and obstacle avoidance constraints.

and

$$\mathbf{B} = \begin{bmatrix} 2(\sin(nT/2))^2/n^2 & -2(\sin(nT)-nT)/n^2 & 0 \\ 2(\sin(nT)-nT)/n^2 & 8(\sin(nT/2))^2/n^2 - 3T^2/2 & 0 \\ 0 & 0 & 2(\sin(nT/2))^2/n^2 \\ \sin(nT)/n & 4(\sin(nT/2))^2/n & 0 \\ -4(\sin(nT/2))^2/n & 4\sin(nT)/n - 3T & 0 \\ 0 & 0 & \sin(nT)/n \end{bmatrix}. \tag{2.7}$$

2.2. Constraints Considering the limitation of the thrust of the tracking spacecraft, the following control constraints are imposed on both of the rendezvous phase and the docking phase: $|\mathbf{u}_t|_\infty \le u_{\max}$, where $|\cdot|_\infty$ denotes the ∞-norm.

During the rendezvous phase, obstacle avoidance is an important mission. For this, we impose the following rotating hyperplane constraint [23]:

$$\mathbf{n}_t^T \mathbf{x}_{p,t} \ge \mathbf{n}_t^T \mathbf{r}_{c,t}, \tag{2.8}$$

where $\mathbf{n}_t$ is the normal vector to the hyperplane, $\mathbf{r}_{c,t}$ is the tangent point between the hyperplane and the obstacle, and $\mathbf{x}_{p,t}$ is the position of the tracking spacecraft at time step t as shown in Figure 2. Obviously, the tracking spacecraft is outside the obstacle as long as (2.8) is satisfied.

REMARK 2.1. During the obstacle avoidance, $\mathbf{n}_t$ and $\mathbf{r}_{c,t}$ are updated at each time instant t. Let N be the length of the prediction horizon. Then, for each $k = 1, 2, \ldots, N$,

https://doi.org/10.1017/S1446181121000031 Published online by Cambridge University Press

the normal vector $\mathbf{n}_{t+k}$ is rotating around the obstacle with a predetermined rotation rate θ_0. In other words, $\mathbf{n}_{t+k+1} = \mathbf{n}_{t+k} + \theta_0$.

If the distance between the tracking spacecraft and the target spacecraft is less than a certain number $d_0 = 2$km, the docking phase begins. In order to prevent the tracking spacecraft colliding with the target spacecraft, the following constraint is imposed:

$$u_{y,t} \le \mu e^{-\beta t}, \tag{2.9}$$

where $\mu > 0$ and $\beta > 0$. When the tracking spacecraft approaches the target spacecraft, inequality (2.9) forces the control input in the y-direction to decrease gradually.

Since there is a limit on the working distance of the sensors on the target spacecraft, as illustrated in Figure 2, we impose the line-of-sight (LoS) cone constraints [13] $\mathbf{A}_{\text{cone}}\mathbf{x}_t \le \mathbf{b}_{\text{cone}}$. An overshoot constraint $\mathbf{x}_{y,t} \ge 0$ is also considered to avoid missing an in-track target.

2.3. SMPC problem In this method, we add the state point set $\mathbf{x_s}$ to the MPC problem formulation, and add a penalty term to the cost. The vectors $\mathbf{x_k}$ and $\mathbf{u_k}$ are state and control vectors to be determined; $\mathbf{x_s}$ and $\mathbf{u_s}$ are the forced equilibrium state and control to be determined. The rendezvous phase is described by

$$\min_{\mathbf{u}_k,\mathbf{x}_s,\mathbf{u}_s} \quad \mathbb{E}_{[\mathbb{P}]}\Bigg\{\sum_{k=t}^{t+N-1} ((\mathbf{x}_k - \mathbf{x}_s)^T\mathbf{Q}(\mathbf{x}_k - \mathbf{x}_s) + (\mathbf{u}_k - \mathbf{u}_s)^T\mathbf{R}(\mathbf{u}_k - \mathbf{u}_s)) + \mathbf{x}_s^T\mathbf{P}\mathbf{x}_s.$$

$$+ (\mathbf{x}_N - \mathbf{x}_s)^T\mathbf{Q}^{\text{final}}(\mathbf{x}_N - \mathbf{x}_s)\Bigg\}, \tag{2.10a}$$

subject to

$$\mathbf{x}_{t+1} = \mathbf{A}\mathbf{x}_t + \mathbf{B}\mathbf{u}_t + \boldsymbol{\delta}_t, \tag{2.10b}$$

$$\mathbf{x}_s = \mathbf{A}\mathbf{x}_s + \mathbf{B}\mathbf{u}_s, \tag{2.10c}$$

$$\Pr_{[\mathbb{P}]}[-\mathbf{n}_{t+k}^T\mathbf{x}_{p,t+k} \le -\mathbf{n}_{t+k}^T\mathbf{r}_{c,t+k}] \ge 1 - \epsilon_x, \quad k = 1, 2, \ldots, N, \tag{2.10d}$$

$$\Pr_{[\mathbb{P}]}[\mathbf{c}_i^T\mathbf{u}_{t+k} \le u_{\max}] \ge 1 - \epsilon_u, \quad k = 0, 1, \ldots, N-1, \; i = 1, 2, \ldots, 6, \tag{2.10e}$$

where $\mathbb{E}_{[\mathbb{P}]}\{\cdot\}$ and $\Pr_{[\mathbb{P}]}[\cdot]$ denote, respectively, the statistical expectation and the probability under the distribution $\mathbb{P}$. In addition, the derivation of (2.10a) is shown in the Appendix.

During the docking phase, obstacle avoidance is no longer considered and the reference governor is removed. In this study, the spacecraft contains only one thruster.

In order to change the thrust direction, the attitude of the spacecraft must be changed. If the thrust direction changes too fast, the attitude controller of the spacecraft will not be able to keep up with commanded thrust direction changes. So, we augment the cost function with a term

$$\sum_{k=t}^{t+N-1} (\mathbf{u}_k - \mathbf{u}_{k-1})^T \tilde{\mathbf{Q}} (\mathbf{u}_k - \mathbf{u}_{k-1}),$$

where $\tilde{\mathbf{Q}} = (\tilde{\mathbf{Q}})^T > 0$ is a weight matrix. Obviously, the thrust direction change will be limited after adding this term. This penalty for the rate at which the thrust vectors change is found to be effective in dealing with the bandwidth and capacity constraints of the attitude controller.

The penalty term of the attitude controller is added, and the overshoot constraint, LoS cone constraints, and thrust direction constraints are added. Thus, the docking phase is described by

$$\min_{\mathbf{u}_k} \quad \mathbb{E}_{[\mathbb{P}]}\Big\{ \sum_{k=t}^{t+N-1} (\mathbf{x}_k^T \mathbf{Q} \mathbf{x}_k + \mathbf{u}_k^T \mathbf{R} \mathbf{u}_k) + \sum_{k=t}^{t+N} (\mathbf{u}_k - \mathbf{u}_{k-1})^T \tilde{\mathbf{Q}} (\mathbf{u}_k - \mathbf{u}_{k-1}) + \mathbf{x}_N^T \mathbf{Q}^{\text{final}} \mathbf{x}_N \Big\}, \tag{2.11a}$$

$$\text{subject to} \quad \mathbf{x}_{t+1} = \mathbf{A}\mathbf{x}_t + \mathbf{B}\mathbf{u}_t + \boldsymbol{\delta}_t, \tag{2.11b}$$

$$\Pr_{[\mathbb{P}]}[\mathbf{A}_{\text{cone}_{i,k}}^T \mathbf{x}_{t+k} \le b_{\text{cone}_i}] \ge 1 - \epsilon_x, \quad k = 1, 2, \ldots, N,\ i = 1, 2, \ldots, 5, \tag{2.11c}$$

$$\Pr_{[\mathbb{P}]}[\mathbf{a}_{6,k}^T \mathbf{x}_{t+k} \le 0] \ge 1 - \epsilon_x, \quad k = 1, 2, \ldots, N, \tag{2.11d}$$

$$\Pr_{[\mathbb{P}]}[\mathbf{c}_{i,k}^T \mathbf{u}_{t+k} \le u_{\max}] \ge 1 - \epsilon_u, \quad k = 0, 1, \ldots, N-1,\ i = 1, 2, \ldots, 6, \tag{2.11e}$$

$$\Pr_{[\mathbb{P}]}[\mathbf{c}_{7,k}^T \mathbf{u}_{t+k} \le \mu e^{-\beta k}] \ge 1 - \epsilon_u, \quad k = 0, 1, \ldots, N-1, \tag{2.11f}$$

where ϵ_x and ϵ_u are design parameters, and $\mathbf{A}_{\text{cone}_i}$ and b_{cone_i} represent line i of $\mathbf{A}_{\text{cone}}$ and b_{cone}, respectively. Since thrust is directional, the thrust constraints include six constraints. And,

$$\mathcal{P} = \{\mathbb{P} \mid \mathbb{E}_{[\mathbb{P}]}[\boldsymbol{\delta}_t] = \boldsymbol{\mu}_{\mathbf{0}}, \mathbb{E}_{[\mathbb{P}]}[(\boldsymbol{\delta}_t - \boldsymbol{\mu}_{\mathbf{0}})(\boldsymbol{\delta}_t - \boldsymbol{\mu}_{\mathbf{0}})^T] = \mathbf{S}_{\mathbf{0}}\}, \tag{2.12}$$

where the predictive horizon and the control horizon are both set as N. Here $\mathbf{Q}$ and $\mathbf{R}$ are the specified weighting matrices, $\mathbf{P}$ is the weighting on the forced equilibrium states, and $\mathbf{Q}^{\text{final}}$ is the terminal weight matrix as calculated by the Riccati equation.

https://doi.org/10.1017/S1446181121000031 Published online by Cambridge University Press

3. SMPC algorithm

As we mentioned earlier, one can find multiple sources of disturbances in space vehicles. In Section 2, we took into account disturbances and system uncertainties, and represented rendezvous and docking as a stochastic optimization problem. However, such a form cannot be calculated. We must convert it into a convex form that can be calculated on-line. We take

$$\mathbf{x} = \begin{bmatrix} \mathbf{x}_t^T \\ \mathbf{x}_{t+1}^T \\ \mathbf{x}_{t+2}^T \\ \cdots \\ \mathbf{x}_{t+N}^T \end{bmatrix}, \quad \mathbf{u} = \begin{bmatrix} \mathbf{u}_t^T \\ \mathbf{u}_{t+1}^T \\ \mathbf{u}_{t+2}^T \\ \cdots \\ \mathbf{u}_{t+N-1}^T \end{bmatrix}, \quad \boldsymbol{\delta} = \begin{bmatrix} \boldsymbol{\delta}_t^T \\ \boldsymbol{\delta}_{t+1}^T \\ \boldsymbol{\delta}_{t+2}^T \\ \cdots \\ \boldsymbol{\delta}_{t+N-1}^T \end{bmatrix}.$$

Thus, we can rewrite the system model into a compact form [5]

$$\mathbf{x} = \mathbf{F}\mathbf{x}_t + \mathbf{G}_u\mathbf{u} + \mathbf{G}_\delta\boldsymbol{\delta},$$

where $\mathbf{F} \in \mathbb{R}^{n_xN\times n_x}$, $\mathbf{G}_u \in \mathbb{R}^{n_x(N+1)\times n_uN}$, and $\mathbf{G}_\delta \in \mathbb{R}^{n_x(N+1)\times n_xN}$, with

$$\mathbf{F} = \begin{bmatrix} \mathbf{I}_{n_x\times n_x} \\ \mathbf{A} \\ \mathbf{A}^2 \\ \vdots \\ \mathbf{A}^N \end{bmatrix}, \quad \mathbf{G}_u = \begin{bmatrix} \mathbf{0}_{n_x\times n_u} & \mathbf{0}_{n_x\times n_u} & \cdots & \mathbf{0}_{n_x\times n_u} \\ \mathbf{B} & \mathbf{0}_{n_x\times n_u} & \cdots & \mathbf{0}_{n_x\times n_u} \\ \mathbf{AB} & \mathbf{B} & \cdots & \mathbf{0}_{n_x\times n_u} \\ \vdots & \vdots & \ddots & \vdots \\ \mathbf{A}^{N-1}\mathbf{B} & \mathbf{A}^{N-2}\mathbf{B} & \cdots & \mathbf{B} \end{bmatrix},$$

$$\mathbf{G}_\delta = \begin{bmatrix} \mathbf{0}_{n_x\times n_x} & \mathbf{0}_{n_x\times n_x} & \cdots & \mathbf{0}_{n_x\times n_x} \\ \mathbf{I}_{n_x\times n_x} & \mathbf{0}_{n_x\times n_x} & \cdots & \mathbf{0}_{n_x\times n_x} \\ \mathbf{A} & \mathbf{I}_{n_x\times n_x} & \cdots & \mathbf{0}_{n_x\times n_x} \\ \vdots & \vdots & \ddots & \vdots \\ \mathbf{A}^{N-1} & \mathbf{A}^{N-2} & \cdots & \mathbf{I}_{n_x\times n_x} \end{bmatrix}.$$

The feedback control law is

$$\mathbf{u}_t = \overline{\mathbf{u}}_t + \mathbf{K}_t(\mathbf{x}_t - \overline{\mathbf{x}}_t), \tag{3.1}$$

where $\overline{\mathbf{u}}_\mathbf{t}$ and $\overline{\mathbf{x}}_\mathbf{t}$ are the state vector and the control vector of the nominal system, respectively, and $\mathbf{K}_t$ is time-varying feedback gain matrix. Equation (3.1) can be rewritten as

$$\mathbf{u} = \boldsymbol{\Theta}\boldsymbol{\delta} + \overline{\mathbf{u}} + \mathbf{K}(\mathbf{x}_\mathbf{t} - \overline{\mathbf{x}}_\mathbf{t}), \tag{3.2}$$

https://doi.org/10.1017/S1446181121000031 Published online by Cambridge University Press

where

$$\bar{\mathbf{u}} = \begin{bmatrix} \bar{\mathbf{u}}_t \\ \vdots \\ \bar{\mathbf{u}}_{t+N-1} \end{bmatrix}, \quad \mathbf{K} = \begin{bmatrix} \mathbf{K}_t \\ \mathbf{K}_{t+1}\boldsymbol{\Psi}_t \\ \mathbf{K}_{t+2}\boldsymbol{\Psi}_{t+1}\boldsymbol{\Psi}_t \\ \vdots \\ \mathbf{K}_{t+N-1}\boldsymbol{\Psi}_{t+N-2}\cdots\boldsymbol{\Psi}_t \end{bmatrix},$$

$$\boldsymbol{\Theta} = \begin{bmatrix} \mathbf{0}_{n_u\times n_x} & \cdots & \mathbf{0}_{n_u\times n_x} & \mathbf{0}_{n_u\times n_x} \\ \mathbf{K}_{t+1} & \cdots & \mathbf{0}_{n_u\times n_x} & \mathbf{0}_{n_u\times n_x} \\ \mathbf{K}_{t+2}\boldsymbol{\Psi}_{t+1} & \cdots & \mathbf{0}_{n_u\times n_x} & \mathbf{0}_{n_u\times n_x} \\ \vdots & \ddots & \vdots & \vdots \\ \mathbf{K}_{t+N-2}\boldsymbol{\Psi}_{t+N-3}\cdots\boldsymbol{\Psi}_{t+1} & \cdots & \mathbf{K}_{t+N-2} & \mathbf{0}_{n_u\times n_x} \\ \mathbf{K}_{t+N-1}\boldsymbol{\Psi}_{t+N-2}\cdots\boldsymbol{\Psi}_{t+1} & \cdots & \mathbf{K}_{t+N-2}\boldsymbol{\Psi}_{t+N-3} & \mathbf{K}_{t+N-1} \end{bmatrix},$$

and $\boldsymbol{\Psi}_t = (\mathbf{A} + \mathbf{B}\mathbf{K}_t)$. For convenience of description, we take $\mathbf{z} = \bar{\mathbf{u}} + \mathbf{K}(\mathbf{x}_t - \bar{\mathbf{x}}_t)$. Therefore, (3.2) can be rewritten as

$$\mathbf{u} = \boldsymbol{\Theta}\delta + \mathbf{z}.$$

3.1. Convex expression of objective function By substituting formula (2.5) into formula (2.10a) and calculating and sorting out formula (2.10a),

$$\min_{\bar{\mathbf{u}},\mathbf{K},\mathbf{P}^*} \quad \mathrm{tr}(\boldsymbol{\Delta}_1\boldsymbol{\Theta}\mathbf{S} + \mathbf{P}^*\mathbf{S}) + (\mathbf{F}\mathbf{x}_t + \mathbf{G}_u\mathbf{z} - \mathbf{X}_s)^T\mathbf{Q}_l(\mathbf{F}\mathbf{x}_t + \mathbf{G}_u\mathbf{z} - \mathbf{X}_s)$$
$$+ (\mathbf{z} - \mathbf{U}_s)^T\mathbf{R}_l(\mathbf{z} - \mathbf{U}_s) + \mathbf{x}_s^T\mathbf{P}\mathbf{x}_s + c, \tag{3.3}$$

where $\mathrm{tr}(\cdot)$ represents the trace of a matrix and $\mathbf{S} = \mathbf{I}_N \otimes \mathbf{S}_0$. Here $\mathbf{I}_N$ denotes an $N \times N$ identity matrix and $\otimes$ denotes the Kronecker product. Also, $\mathbf{P}^* = \boldsymbol{\Theta}^T\boldsymbol{\Delta}_2\boldsymbol{\Theta} \geq 0$, $\mathbf{y} = \mathbf{F}\mathbf{x}_t + \mathbf{G}_u\mathbf{z}$, $\boldsymbol{\Delta}_1 = 2\mathbf{G}_\delta^T\mathbf{Q}_l\mathbf{G}_u$, $\boldsymbol{\Delta}_2 = \mathbf{R}_l + \mathbf{G}_u^T\mathbf{Q}_l\mathbf{G}_u$, $c = \mathrm{tr}(\mathbf{G}_\delta^T\mathbf{Q}_l\mathbf{G}_\delta\mathbf{S})$, $\mathbf{Q}_l \in \mathbb{R}^{n_x(N+1)\times n_x(N+1)}$, $\mathbf{R}_l \in \mathbb{R}^{n_uN\times n_uN}$,

$$\mathbf{Q}_l = \begin{bmatrix} \mathbf{Q} & \mathbf{0} & \cdots & \mathbf{0} \\ \mathbf{0} & \mathbf{Q} & \cdots & \mathbf{0} \\ \vdots & \vdots & \ddots & \vdots \\ \mathbf{0} & \mathbf{0} & \cdots & \mathbf{Q}^{\mathrm{final}} \end{bmatrix}, \quad \mathbf{R}_l = \begin{bmatrix} \mathbf{R} & \mathbf{0} & \cdots & \mathbf{0} \\ \mathbf{0} & \mathbf{R} & \cdots & \mathbf{0} \\ \vdots & \vdots & \ddots & \vdots \\ \mathbf{0} & \mathbf{0} & \cdots & \mathbf{R} \end{bmatrix},$$

$\mathbf{X}_s \in \mathbb{R}^{n_x(N+1)\times n_x}$, $\mathbf{U}_s \in \mathbb{R}^{n_uN\times n_u}$, $\mathbf{X}_s = \mathbf{1}_N \otimes \mathbf{x}_s$, and $\mathbf{U}_s = \mathbf{1}_N \otimes \mathbf{u}_s$. In addition, we put the derivation of formula (3.3) in the Appendix.

By substituting formula (2.5) into formula (2.11a) and calculating and integrating formula (2.11a),

$$\min_{\bar{\mathbf{u}},\mathbf{K},\mathbf{P}^*} \quad \mathrm{tr}(\boldsymbol{\Delta}_1\boldsymbol{\Theta}\mathbf{S}) + \mathbf{z}^T\boldsymbol{\Delta}_2\mathbf{z} + 2(\mathbf{F}\mathbf{x}_t)^T\mathbf{Q}_l\mathbf{G}_u\mathbf{z} + (\mathbf{F}\mathbf{x}_t)^T\mathbf{Q}_l(\mathbf{F}\mathbf{x}_t) + c + \mathrm{tr}(\mathbf{P}^*\mathbf{S})$$
$$+ (\bar{\mathbf{u}} - \bar{\mathbf{u}}_{-1})^T\mathbf{R}_a(\bar{\mathbf{u}} - \bar{\mathbf{u}}_{-1}), \tag{3.4}$$

https://doi.org/10.1017/S1446181121000031 Published online by Cambridge University Press

where $\mathbf{R}_a \in \mathbb{R}^{n_u N \times n_u N}$,

$$\bar{\mathbf{u}}_{-1} = \begin{bmatrix} \bar{\mathbf{u}}_{t-1} \\ \vdots \\ \bar{\mathbf{u}}_{t+N-1} \end{bmatrix}, \quad \bar{\mathbf{u}} = \begin{bmatrix} \bar{\mathbf{u}}_{t} \\ \vdots \\ \bar{\mathbf{u}}_{t+N} \end{bmatrix}, \quad \mathbf{R}_a = \begin{bmatrix} \tilde{\mathbf{Q}} & \cdots & \mathbf{0}_{n_u \times n_u} \\ \vdots & \ddots & \vdots \\ \mathbf{0}_{n_u \times n_u} & \cdots & \tilde{\mathbf{Q}} \end{bmatrix}.$$

In addition, the derivation of formula (3.4) is similar to that of formula (3.3) and will not be repeated here. We can find a way to deal with probabilistic constraints [6].

LEMMA 3.1. *For any $\epsilon \in (0, 1)$, the distributionally robust chance constraint*

$$\inf_{d\ (\hat{d},\Gamma)} \Pr[d^T \tilde{x} \leq 0] \geq 1 - \epsilon_x$$

is equivalent to the convex second-order cone constraint

$$\sqrt{\frac{1-\epsilon}{\epsilon}} \tilde{x}^T \Sigma \tilde{x} + \mu^T \tilde{x} \leq 0,$$

where

$$\mathcal{P} = \{\mathbb{P} \mid \mathbb{E}_{[\mathbb{P}]}[\tilde{x}] = \mu,\ \mathbb{E}_{[\mathbb{P}]}[(\tilde{x} - \mu)(\tilde{x} - \mu)^T] = S\}.$$

Using Lemma 3.1, we can transform (2.10d) and (2.10e) into

$$\sqrt{\frac{1-\epsilon_x}{\epsilon_x}} \| - S_0^{1/2} \mathbf{\Pi}^T \mathbf{n}_{t+k} \| \leq -\mathbf{n}_{t+k}^T \mathbf{r}_{c,t+k} + \mathbf{n}_{t+k}^T \mathbf{y}, \quad k = 1, 2, \ldots, N,$$

$$\sqrt{\frac{1-\epsilon_u}{\epsilon_u}} \| S_0^{1/2} \mathbf{\Theta} \mathbf{c}_{i,k} \| \leq u_{\max} - \mathbf{c}_{i,k}^T \mathbf{z}, \quad k = 0, 1, \ldots, N-1, i = 1, 2, \ldots, 6,$$

where $\mathbf{\Pi} = \mathbf{G}_u \mathbf{\Theta} + \mathbf{G}_\delta$. Using similar methods to deal with (2.11d)–(2.11f),

$$\sqrt{\frac{1-\epsilon_x}{\epsilon_x}} \| S_0^{1/2} \mathbf{\Pi}^T \mathbf{A}_{\mathrm{cone}_{i,k}} \| \leq b_{\mathrm{cone}_i} - \mathbf{a}_{i,k}^T \mathbf{y}, \quad k = 1, 2, \ldots, N,\ i = 1, 2, \ldots, 5,$$

$$\sqrt{\frac{1-\epsilon_x}{\epsilon_x}} \| S_0^{1/2} \mathbf{\Pi}^T \mathbf{a}_{6,k} \| \leq -\mathbf{a}_{6,k}^T \mathbf{y}, \quad k = 1, 2, \ldots, N,$$

$$\sqrt{\frac{1-\epsilon_u}{\epsilon_u}} \| S_0^{1/2} \mathbf{\Theta} \mathbf{c}_{i,k} \| \leq u_{\max} - \mathbf{c}_{i,k}^T \mathbf{z}, \quad k = 0, 1, \ldots, N-1,\ i = 1, 2, \ldots, 6,$$

$$\sqrt{\frac{1-\epsilon_u}{\epsilon_u}} \| S_0^{1/2} \mathbf{\Theta} \mathbf{c}_{7,k} \| \leq \mu e^{-\beta k} - \mathbf{c}_{7,k}^T \mathbf{z}, \quad k = 0, 1, \ldots, N-1.$$

https://doi.org/10.1017/S1446181121000031 Published online by Cambridge University Press

3.2. Strategy of initialization

REMARK 3.2. In our previous work, two strategies were proposed.

STRATEGY 1. Reset of the initial state: in the MPC optimization problem set $\bar{\mathbf{x}}_{t|t} = \mathbf{x}_t$.

STRATEGY 2. Prediction: in the MPC optimization problem set $\bar{\mathbf{x}}_{t|t} = \bar{\mathbf{x}}_{t|t-1}$.

So far, all problems have been transformed into convex forms and we can use other tools to solve this problem. During the rendezvous phase,

$$\begin{aligned}
\min_{\bar{\mathbf{u}},\mathbf{K},\mathbf{P}^*} \quad & \mathrm{tr}(\boldsymbol{\Delta}_1\boldsymbol{\Theta}\mathbf{S} + \mathbf{P}^*\mathbf{S}) + (\mathbf{F}\mathbf{x}_t + \mathbf{G}_u\mathbf{z} - \mathbf{X}_s)^T\mathbf{Q}_l(\mathbf{F}\mathbf{x}_t + \mathbf{G}_u\mathbf{z} - \mathbf{X}_s) \\
& + (\mathbf{z} - \mathbf{U}_s)^T\mathbf{R}_l(\mathbf{z} - \mathbf{U}_s) + \mathbf{x}_s^T\mathbf{P}\mathbf{x}_s + c, \qquad (3.5\text{a})
\end{aligned}$$

$$\text{subject to} \quad \sqrt{\frac{1-\epsilon_x}{\epsilon_x}}\| - S_0^{1/2}\boldsymbol{\Pi}^T\mathbf{n}_{t+k}\| \le -\mathbf{n}_{t+k}^T\mathbf{r}_{c,t+k} + \mathbf{n}_{t+k}^T\mathbf{y}, \quad k = 1,2,\ldots,N, \qquad (3.5\text{b})$$

$$\sqrt{\frac{1-\epsilon_u}{\epsilon_u}}\|S_0^{1/2}\boldsymbol{\Theta}\mathbf{c}_{i,k}\| \le u_{\max} - \mathbf{c}_{i,k}^T\mathbf{z}, \quad k = 0,1,\ldots,N-1, \; i = 1,2,\ldots,6.$$

During the docking phase,

$$\begin{aligned}
\min_{\bar{\mathbf{u}},\mathbf{K},\mathbf{P}^*} \quad & 2\mathrm{tr}(\boldsymbol{\Delta}_1\boldsymbol{\Theta}\mathbf{S}) + \mathbf{z}^T\boldsymbol{\Delta}_2\mathbf{z} + 2(\mathbf{F}\mathbf{x}_t)^T\mathbf{Q}_l\mathbf{G}_u\mathbf{z} + (\mathbf{F}\mathbf{x}_t)^T\mathbf{Q}_l(\mathbf{F}\mathbf{x}_t) + \mathrm{tr}(\mathbf{G}_\delta^T\mathbf{Q}_l\mathbf{G}_\delta) \\
& + \mathrm{tr}(\mathbf{P}^*\mathbf{S}) + (\bar{\mathbf{u}} - \bar{\mathbf{u}}_{-1})^T\mathbf{R}_a(\bar{\mathbf{u}} - \bar{\mathbf{u}}_{-1}),
\end{aligned}$$

$$\begin{aligned}
\text{subject to} \quad & \sqrt{\frac{1-\epsilon_x}{\epsilon_x}}\|S_0^{1/2}\boldsymbol{\Pi}^T\mathbf{A}_{\mathrm{cone}_{i,k}}\| \le b_{\mathrm{cone}_i} - \mathbf{a}_{i,k}^T\mathbf{y}, \quad k = 1,2,\ldots,N, \; i = 1,2,\ldots,5, \\
& \sqrt{\frac{1-\epsilon_x}{\epsilon_x}}\|S_0^{1/2}\boldsymbol{\Pi}^T\mathbf{a}_{6,k}\| \le -\mathbf{a}_{6,k}^T\mathbf{y}, \quad k = 1,2,\ldots,N, \\
& \sqrt{\frac{1-\epsilon_u}{\epsilon_u}}\|S_0^{1/2}\boldsymbol{\Theta}\mathbf{c}_{i,k}\| \le u_{\max} - \mathbf{c}_{i,k}^T\mathbf{z}, \quad k = 0,1,\ldots,N-1, \; i = 1,2,\ldots,6, \\
& \sqrt{\frac{1-\epsilon_u}{\epsilon_u}}\|S_0^{1/2}\boldsymbol{\Theta}\mathbf{c}_{7,k}\| \le \mu e^{-\beta k} - \mathbf{c}_{7,k}^T\mathbf{z}, \quad k = 0,1,\ldots,N-1.
\end{aligned}$$

4. Simulation results

All simulation results were obtained on a 2.2-GHz Intel Core i7 processor. MATLAB 2018a and CVX [14] toolbox were used for simulation. The target spacecraft is in a nominal circular orbit at an altitude of 850 km above the Earth, that is, $n = 0.0255$. The control horizon and the prediction horizon N are fixed at four steps. Concerning the constraints, the maximum amount of acceleration that the chaser's

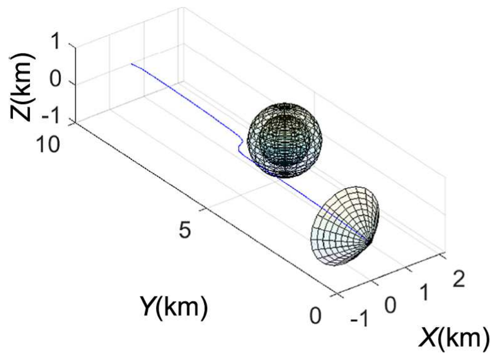

FIGURE 3. MPC path simulation without disturbance.

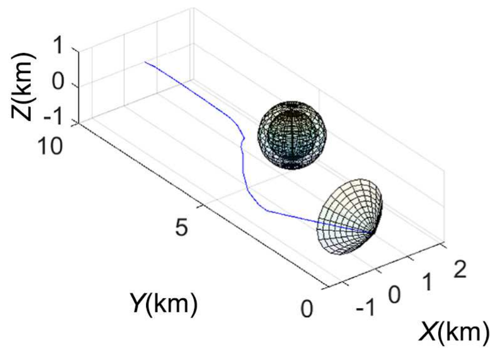

FIGURE 4. RMPC path simulation without disturbance.

actuators can provide is $u_{\max} = 4\ \mathrm{m/s^2}$. The obstacle avoidance hyperplane rotates counter clockwise (viewed from the $+Z$ direction of Hill's frame) at a speed of 30°/min.

The corresponding weight matrices are $\mathbf{R} = 2\times 10^5\mathbf{I}_3$, $\mathbf{R}_a = 2\times 10^6\mathbf{I}_3$, $\mathbf{Q} = \mathrm{diag}(10^2, 10^2, 10^2, 10^7, 10^7, 10^7)$, $\mathbf{P} = 10^7\mathbf{I}_6$. An obstacle is introduced during the rendezvous phase at $r_0 = (1.3, 5, 0)$ km, and the initial radius of the uncertain sphere is 0.6 km, increasing by 0.03 km per minute. Here $\epsilon_x = \epsilon_u = 0.05$, $\mu = 10^{-2}$, and $\beta = 5$. In addition, a Monte Carlo analysis was conducted to get more confidence on the controller design. Two hundred simulations were performed for MPC, RMPC, and SMPC.

The simulation results of MPC, RMPC, and SMPC without disturbance are given in Figures 3, 4, and 5, respectively, and the initial position of the tracking spacecraft is $x_0 = (0.63, 10, 0)$ km. It can be seen from the figures that all three methods can be successfully docked without disturbance. As shown in Figure 3, since the other two methods are more conservative, the standard MPC has a more efficient path.

We assume that the disturbance is a Gaussian disturbance with mean value of 0 and variance of 8×10^{-4}. Results for MPC simulations are shown in Figure 6, results for RMPC simulations are shown in Figure 7, and results for SMPC simulations are shown

https://doi.org/10.1017/S1446181121000031 Published online by Cambridge University Press

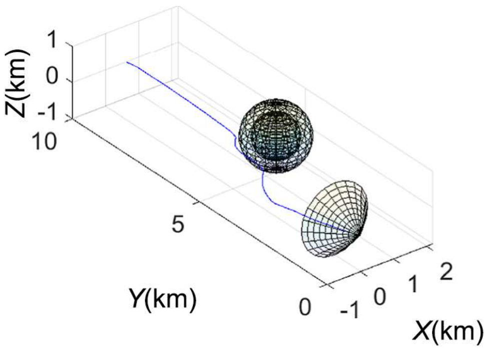

FIGURE 5. SMPC path simulation without disturbance.

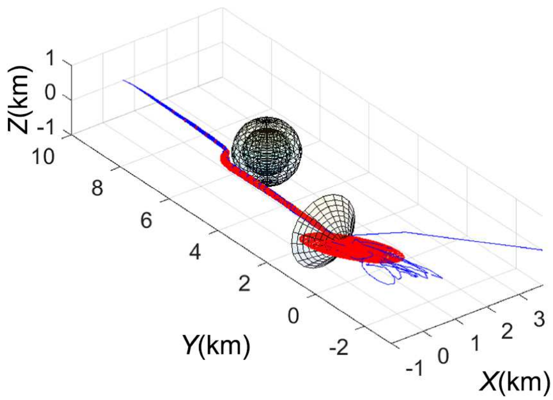

FIGURE 6. MPC path simulation with Gaussian perturbation.

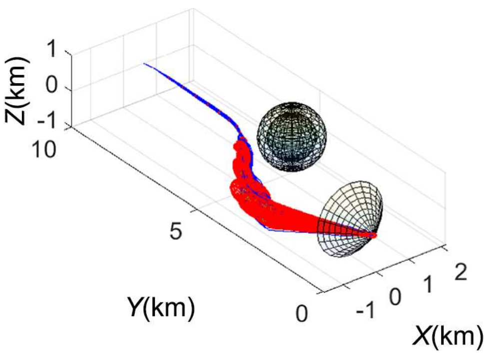

FIGURE 7. RMPC path simulation with Gaussian perturbation.

https://doi.org/10.1017/S1446181121000031 Published online by Cambridge University Press

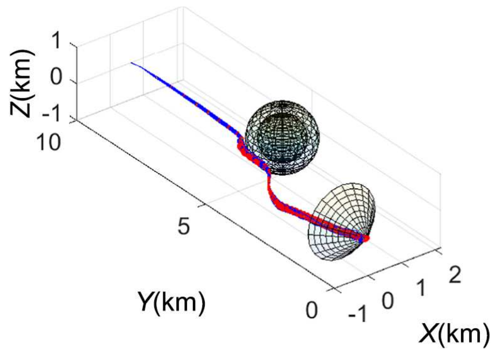

FIGURE 8. SMPC path simulation with Gaussian perturbation.

TABLE 1. The number of docking failures of the three methods.

	MPC	RMPC	SMPC
Gaussian perturbation	21	0	0
Laplace perturbation	40	0	0

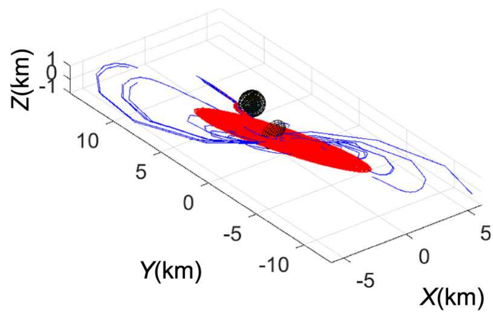

FIGURE 9. MPC path simulation with Laplace perturbation.

in Figure 8. Note that in all the simulation results of this paper, the red area represents the confidence interval. As shown in Figure 6, the standard MPC may not succeed in the presence of disturbances (that is, it failed to reach the origin). We counted the number of docking failures of the three methods and show it in Table 1. In addition, as shown in Figure 7, the results for RMPC are more conservative.

In order to make the results more convincing, we set the disturbance as a Laplace distribution and simulated it and the results are shown in Figures 9, 10, and 11. It can be seen that the results are basically consistent with that of the Gaussian distribution. Similarly, we counted the number of docking failures of the three methods and show it in Table 1. It can be seen that the standard MPC has docking failure when there is a disturbance, while RMPC and SMPC can ensure successful docking.

https://doi.org/10.1017/S1446181121000031 Published online by Cambridge University Press

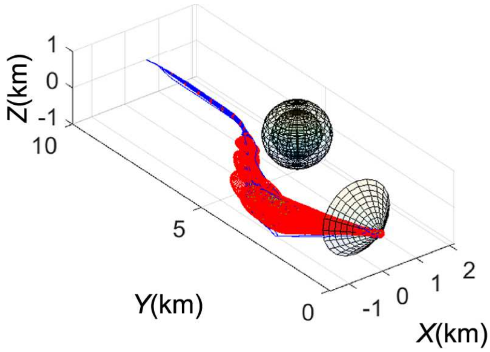

FIGURE 10. RMPC path simulation with Laplace perturbation.

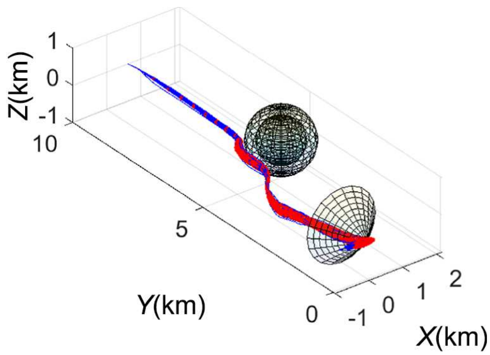

FIGURE 11. SMPC path simulation with Laplace perturbation.

TABLE 2. Total fuel consumption of three methods.

	MPC (J/kg)	RMPC (J/kg)	SMPC (J/kg)
Gaussian perturbation	0.0018	0.0327	0.0104
Laplace perturbation	0.0101	0.0326	0.0116

More importantly, we must point out that the fuel consumption of RMPC is larger because of its conservatism, while SMPC has less fuel consumption when ensuring the docking success, which is very important for engineering practice, because the fuel that the spacecraft can carry is very limited and adding fuel is troublesome. We calculated the average fuel consumption of the three methods in 200 simulations (including failed attempts) under the two disturbances and show it in Table 2, which will demonstrate our conclusion, where J is the unit of heat.

We see that when the disturbance is the Laplace distribution, the MPC fuel consumption is more than that when the disturbance is the Gaussian distribution, which is because the MPC docking failures are more under the Laplace distribution.

TABLE 3. The control law computation time of three methods.

	MPC (s)	RMPC (s)	SMPC (s)
Rendezvous phase	0.4	0.5	1.2
Docking phase	0.5	0.6	1.6

In addition, in order to demonstrate the computational complexity of SMPC, the control law computation times of the three methods in the rendezvous phase and the docking phase are listed in Table 3.

From Table 3, we can see that although the control law computation time of SMPC is longer than the other two methods, it is still acceptable compared with the sampling time of 20 s.

5. Conclusions

Autonomous spacecraft rendezvous and docking manoeuvres are very important to the aerospace industry, and they have high technical requirements. In particular, it is very difficult to improve the autonomy of spacecraft from the perspective of control theory. Therefore, we must propose better solutions to enable the spacecraft to deal with various unmodelled disturbances under various constraints. At the same time, the fuel consumption of the spacecraft is reduced to a minimum.

In this paper, a stochastic model predictive controller with chance constraints is proposed. The Clohessy–Wiltshire–Hill model with unbounded disturbances and various constraints is used to solve the problem of spacecraft rendezvous and docking. The simulation results show that SMPC has the ability to deal with disturbances and the computational complexity is acceptable. Specifically, compared with the standard MPC, SMPC can ensure the successful docking of spacecraft, and SMPC has less fuel consumption compared with RMPC, which is very important for engineering practice.

Appendix

After substituting the system equations (2.5), (2.10a) is rewritten as

$$\begin{aligned}
&(\mathbf{F}\mathbf{x}_t)^T\mathbf{Q}_l(\mathbf{F}\mathbf{x}_t) + 2(\mathbf{F}\mathbf{x}_t)^T\mathbf{Q}_l\mathbf{G}_u\mathbb{E}_{[\mathbb{P}]}[\mathbf{u}] \\
&\quad + 2(\mathbf{F}\mathbf{x}_t)^T\mathbf{Q}_l(\mathbf{G}_\delta\mathbb{E}_\mathbb{P}[\boldsymbol{\delta}]) - 2(\mathbf{F}\mathbf{x}_t)^T\mathbf{Q}_l\mathbf{X}_s \\
&\quad + \mathbb{E}_\mathbb{P}[\mathbf{u}^T(\mathbf{R}_l + \mathbf{G}_u\mathbf{Q}_l\mathbf{G}_u)\mathbf{u}] + 2\mathbb{E}_\mathbb{P}[(\mathbf{G}_u\mathbf{u})^T\mathbf{Q}_l(\mathbf{G}_\delta\boldsymbol{\delta})] \\
&\quad - 2(\mathbf{G}_u\mathbb{E}_\mathbb{P}[\mathbf{u}])^T\mathbf{Q}_l\mathbf{X}_s + \mathbb{E}_\mathbb{P}[(\mathbf{G}_\delta\boldsymbol{\delta})^T\mathbf{Q}_l(\mathbf{G}_\delta\boldsymbol{\delta})] \\
&\quad - 2(\mathbf{G}_\delta\mathbb{E}_\mathbb{P}[\boldsymbol{\delta}])^T\mathbf{Q}_l\mathbf{X}_s + \mathbf{X}_s^T\mathbf{Q}_l\mathbf{X}_s + \mathbf{x}_s\mathbf{P}\mathbf{x}_s \\
&\quad + \mathbb{E}_\mathbb{P}[\mathbf{u}^T\mathbf{R}_l\mathbf{u}] - 2\mathbb{E}_\mathbb{P}[\mathbf{u}]^T\mathbf{R}_l\mathbf{U}_s + \mathbf{U}_s^T\mathbf{R}_l\mathbf{U}_s.
\end{aligned} \tag{A.1}$$

https://doi.org/10.1017/S1446181121000031 Published online by Cambridge University Press

In this paper, we set $\mathbb{E}_{[\mathbb{P}]}[\delta] = \mu = \mathbf{0}$, $\mathbb{E}_{[\mathbb{P}]}[\delta\delta^T] = \mathbf{S}$. So,

$$\begin{aligned}(\mathbf{F}\mathbf{x}_t)^T\mathbf{Q}_l\mathbf{G}_u\mathbb{E}_{[\mathbb{P}]}[\mathbf{u}] &= (\mathbf{F}\mathbf{x}_t)^T\mathbf{Q}_l\mathbf{G}_u\mathbb{E}_{[\mathbb{P}]}[\boldsymbol{\Theta}\delta + \mathbf{z}]\\ &= (\mathbf{F}\mathbf{x}_t)^T\mathbf{Q}_l\mathbf{G}_u\mathbf{z},\end{aligned} \tag{A.2}$$

$$\begin{aligned}\mathbb{E}_{[\mathbb{P}]}[\mathbf{u}^T(\mathbf{R}_l + \mathbf{G}_u\mathbf{Q}_l\mathbf{G}_u)\mathbf{u}] &= \mathbb{E}_{[\mathbb{P}]}[(\boldsymbol{\Theta}\delta + \mathbf{z})^T(\mathbf{R}_l + \mathbf{G}_u\mathbf{Q}_l\mathbf{G}_u)(\boldsymbol{\Theta}\delta + \mathbf{z})]\\ &= \mathbb{E}_{[\mathbb{P}]}[\delta^T\boldsymbol{\Theta}^T(\mathbf{R}_l + \mathbf{G}_u^T\mathbf{Q}_l\mathbf{G}_u)\boldsymbol{\Theta}\delta] + \mathbf{z}^T(\mathbf{R}_l + \mathbf{G}_u^T\mathbf{Q}_l\mathbf{G}_u)\mathbf{z}\\ &\quad + 2\mathbb{E}_{[\mathbb{P}]}[\delta^T]\boldsymbol{\Theta}^T(\mathbf{R}_l + \mathbf{G}_u^T\mathbf{Q}_l\mathbf{G}_u)\mathbf{z}\\ &= \mathrm{tr}(\boldsymbol{\Theta}^T(\mathbf{R}_l + \mathbf{G}_u^T\mathbf{Q}_l\mathbf{G}_u)\boldsymbol{\Theta}\mathbf{S}) + \mu^T\boldsymbol{\Theta}^T(\mathbf{R}_l + \mathbf{G}_u^T\mathbf{Q}_l\mathbf{G}_u)\boldsymbol{\Theta}\mu\\ &\quad + \mathbf{z}^T(\mathbf{R}_l + \mathbf{G}_u^T\mathbf{Q}_l\mathbf{G}_u)\mathbf{z} + 2\mu\boldsymbol{\Theta}(\mathbf{R}_l + \mathbf{G}_u^T\mathbf{Q}_l\mathbf{G}_u)\mathbf{z},\end{aligned}$$

$$\begin{aligned}\mathbb{E}_{[\mathbb{P}]}[(\mathbf{G}_u\mathbf{u})^T\mathbf{Q}_l(\mathbf{G}_\delta\delta)] &= \mathbb{E}_{[\mathbb{P}]}[\delta^T\mathbf{G}_\delta^T\mathbf{Q}_l\mathbf{G}_u(\boldsymbol{\Theta}\delta + \mathbf{z})]\\ &= \mathrm{tr}(\mathbf{G}_\delta^T\mathbf{Q}_l\mathbf{G}_u\boldsymbol{\Theta}\mathbf{S}) + \mu^T\mathbf{G}_\delta^T\mathbf{Q}_l\mathbf{G}_u\mathbf{z} + \mu^T\mathbf{G}_\delta^T\mathbf{Q}_l\mathbf{G}_u\boldsymbol{\Theta}\mu,\end{aligned}$$

$$\begin{aligned}&(\mathbf{G}_u\mathbb{E}_{[\mathbb{P}]}[\mathbf{u}])^T\mathbf{Q}_l\mathbf{X}_s = (\mathbf{G}_u\mathbb{E}_{[\mathbb{P}]}[\boldsymbol{\Theta}\delta + \mathbf{z}])^T\mathbf{Q}_l\mathbf{X}_s = (\mathbf{G}_u\mathbf{z})^T\mathbf{Q}_l\mathbf{X}_s,\\ &\mathbb{E}_{\mathbb{P}}(\mathbf{G}_\delta\delta)^T\mathbf{Q}_l(\mathbf{G}_\delta\delta) = \mathrm{tr}(\mathbf{G}_\delta^T\mathbf{Q}_l\mathbf{G}_\delta\mathbf{S}),\end{aligned}$$

$$\mathbb{E}_{[\mathbb{P}]}[\mathbf{u}]^T\mathbf{R}_l\mathbf{U}_s = \mathbb{E}_{[\mathbb{P}]}[(\boldsymbol{\Theta}\delta + \mathbf{z})^T]\mathbf{R}_l U_s = \mathbf{z}^T\mathbf{R}_l\mathbf{U}_s. \tag{A.3}$$

Substituting formulas (A.2)–(A.3) into formula (A.1) and sorting it out, formula (3.3) can be obtained.

Acknowledgement

This work is supported by the National Natural Science Foundation of China under grant no. 61903312.

References

[1] K. T. Alfriend, S. R. Vadali, P. Gurfil, J. P. How and L. S. Breger, *Spacecraft formation flying*, (Elsevier, Oxford, 2010); doi:10.1016/C2009-0-17485-8.

[2] I. Batina, A. A. Stoorvogel and S. Weiland, "Stochastic disturbance rejection in model predictive control by randomized algorithms", Proc. *2001* Amer. *Control Conf. (Cat. No. 01CH37148)*, Arlington, VA, 25–27 June 2001, (IEEE, Arlington, VA, 2001) 732–737; doi:10.1109/ACC.2001.945802.

[3] L. Blackmore, M. Ono, A. Bektassov and B. C. Williams, "A probabilistic particle-control approximation of chance-constrained stochastic predictive control", *IEEE Trans. Robot.* **26** (2010) 502–517; doi:10.1109/TRO.2010.2044948.

[4] S. D. Cairano, H. Park and I. Kolmanovsky, "Model predictive control approach for guidance of spacecraft rendezvous and proximity maneuvering", *Internat. J. Robust Nonlinear Control* **22** (2012) 1398–1427; doi:10.1002/rnc.2827.

[5] G. C. Calafiore and L. Fagiano, "Robust model predictive control via scenario optimization", *IEEE Trans. Automat. Contr.* **58** (2012) 219–224; doi:10.1109/tac.2012.2203054.

[6] G. C. Calafiore and L. E. Ghaoui, "On distributionally robust chance-constrained linear programs", *J. Optim. Theory Appl.* **130** (2006) 1–22; doi:10.1007/s10957-006-9084-x.

[7] E. F. Camacho and C. Bordons, *Model predictive control*, (Springer, London, 1999); doi:10.1007/978-1-4471-3398-8.

[8] M. Cannon, B. Kouvaritakis and X. J. Wu, “Model predictive control for systems with stochastic multiplicative uncertainty and probabilistic constraints”, *Automatica* **45** (2009) 167–172; doi:10.1016/j.automatica.2008.06.017.

[9] E. T. Carter, “State transition matrices for terminal rendezvous studies: brief survey and new example”, *J. Guid. Control Dynam.* **21** (1998) 148–155; doi:10.2514/2.4211.

[10] G. Deaconu, C. Louembet and A. Theron, “Minimizing the effects of navigation uncertainties on the spacecraft rendezvous precision”, *J. Guid. Control Dynam.* **37** (2014) 695–700; doi:10.2514/1.62219.

[11] M. Farina, L. Giulioni and R. Scattolini, “Stochastic linear model predictive control with chance constraints – a review”, *J. Process Control* **44** (2016) 53–67; doi:10.1016/j.jprocont.2016.03.005.

[12] W. Fehse, *Automated rendezvous and docking of spacecraft*, (Cambridge University Press, Cambridge, 2003); doi:10.1017/CBO9780511543388.

[13] F. Gavilan, R. Vazquez and E. F. Camacho, “Chance-constrained model predictive control for spacecraft rendezvous with disturbance estimation”, *Control Eng. Pract.* **20** (2012) 111–122; doi:10.1016/j.conengprac.2011.09.006.

[14] M. Grant and S. Boyd, *CVX: Matlab software for disciplined convex programming*, version 2.1, 2014.

[15] E. N. Hartley, P. A. Trodden, A. G. Richards and J. M. Maciejowski, “Model predictive control system design and implementation for spacecraft rendezvous”, *Control Eng. Pract.* **20** (2012) 695–713; doi:10.1016/j.conengprac.2012.03.009.

[16] J. P. How and M. Tillerson, “Analysis of the impact of sensor noise on formation flying control”, *Proc. 2001 Amer. Control Conf. (Cat. No. 01CH37148)*, Arlington, VA, 25–27 June 2001, (IEEE, Arlington, VA, 2001) 3986–3991; doi:10.1109/ACC.2001.946298.

[17] B. Y. Jiang, Q. L. Hu and M. I. Friswell, “Fixed-time rendezvous control of spacecraft with a tumbling target under loss of actuator effectiveness”, *IEEE Trans. Aerosp. Electron. Syst.* **52** (2016) 1576–1586; doi:10.1109/TAES.2016.140406.

[18] P. Li and Z. H. Zhu, “Model predictive control for spacecraft rendezvous in elliptical orbit”, *Acta Astronaut.* **146** (2018) 339–348; doi:10.1016/j.actaastro.2018.03.025.

[19] R. Liu, Z. W. Sun and D. Ye, “Adaptive sliding mode control for spacecraft autonomous rendezvous with elliptical orbits and thruster faults”, *IEEE Access* **5** (2017) 24853–24862; doi:10.1109/ACCESS.2017.2767179.

[20] A. Miele, M. W. Weeks and M. Ciarcià, “Optimal trajectories for spacecraft rendezvous”, *J. Optim. Theory Appl.* **132** (2007) 353–376; doi:10.1007/s10957-007-9166-4.

[21] S. Nolet, E. Kong, and D. W. Miller, “Autonomous docking algorithm development and experimentation using the SPHERES testbed”, *Proc. SPIE, Vol. 5419, Spacecraft Platforms and Infrastructure*, Orlando, FL, 30 August 2004, (Society of Photographic Instrumentation Engineers – SPIE, Orlando, FL, 2004) 1–15; doi:10.1117/12.547430.

[22] P. K. C. Wang and F. Y. Hadaegh, “Formation flying of multiple spacecraft with autonomous rendezvous and docking capability”, *IET Control Theory Appl.* **1** (2007) 494–504; doi:10.1049/iet-cta:20050411.

[23] A. Weiss, M. Baldwin, R. S. Erwin and I. Kolmanovsky, “Model predictive control for spacecraft rendezvous and docking: strategies for handling constraints and case studies”, *IEEE Trans. Control Syst. Technol.* **23** (2015) 1638–1647; doi:10.1109/TCST.2014.2379639.

[24] B. Wie, *Space vehicle dynamics and control*, (American Institute of Aeronautics and Astronautics, Reston, VA, 1998); doi:10.2514/4.103803.

[25] D. C. Woffinden and D. K. Geller, “Navigating the road to autonomous orbital rendezvous”, *J. Spacecr. Rockets* **44** (2007) 898–909; doi:10.2514/1.30734.

[26] S. Y. Zhu, R. Sun, J. L. Wang, J. H. Wang and X. W. Shao, “Robust model predictive control for multi-step short range spacecraft rendezvous”, *Adv. Space Res.* **62** (2018) 111–126; doi:10.1016/j.asr.2018.03.037.